Biology of Reproduction, 2021, 105(4), 859–875
https://doi.org/10.1093/biolre/ioab109
Research Article
Advance Access Publication Date: 9 June 2021

Research Article

Loss of basigin expression in uterine cells leads to subfertility in female mice†

Kailiang Li[1], Quanxi Li[2], Shah Tauseef Bashir[1], Brent M. Bany[3] and Romana A. Nowak[1,*]

[1]Department of Animal Sciences, University of Illinois at Urbana-Champaign, Urbana, IL, USA, [2]Department of Comparative Biosciences, University of Illinois at Urbana-Champaign, Urbana, IL, USA and [3]Department of Physiology, Southern Illinois University School of Medicine, Carbondale, IL, USA

*__Correspondence:__ Department of Animal Sciences, 310 ASL, 1207 W. Gregory Dr., Urbana, IL 61801, USA.
Tel: 217-244-3902; Fax: 217-333-8286; E-mail: ranowak@uiuc.edu

†__Grant Support:__ This work was supported by NIH HD40093 (RAN) and an Arnold Beckman Award from the University of Illinois (RAN).

Received 19 July 2020; Revised 7 April 2020; Accepted 27 May 2021

Abstract

Basigin (BSG) is a transmembrane glycoprotein involved in cell proliferation, angiogenesis, and tissue remodeling. BSG has been shown to be essential for male and female reproduction although little is known about its role in normal uterine function. To study the potential function of BSG in the female reproductive tract, we generated mice with conditional knockout of Bsg in uterine cells using progesterone receptor-Cre and hypothesized that BSG is required for normal pregnancy in mice. Fertility study data showed that the conditional knockout mice had significantly reduced fertility compared to controls. Ovarian function of the conditional knockout mice appeared normal with no difference in the number of superovulated oocytes collected or in serum progesterone levels between the conditional knockout and the control mice. Uterine tissues collected at various times of gestation showed increased abnormalities in implantation, decidualization, placentation, and parturition in the conditional knockout mice. Uterine cross sections on Day 5 of pregnancy showed implantation failure and abnormal uterine epithelial differentiation in a large proportion of the conditional knockout mice. There was a compromised decidual response to artificial decidualization stimuli and decreased mRNA and protein levels for decidualization genes in the uteri of the conditional knockout mice. We also observed altered protein expression of monocarboxylate transporter 1 (MCT1), as well as impaired angiogenesis in the conditional knockout uteri compared to the controls. These results support that BSG is required for successful pregnancy through its functions in implantation and decidualization.

Summary sentence

Loss of Bsg expression in the uterus leads to subfertility in mice due to impaired implantation and decidualization.

Graphical Abstract

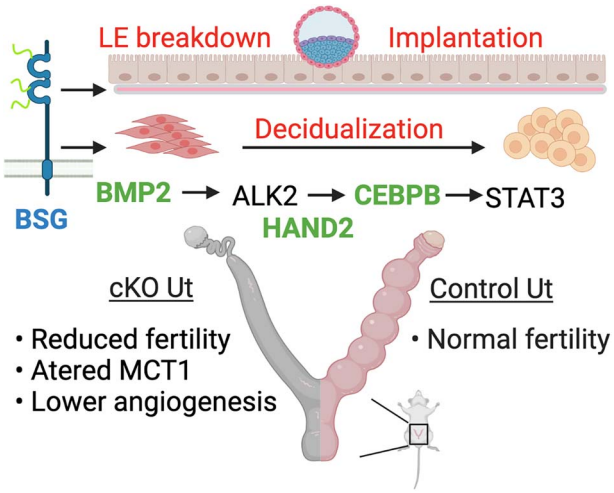

Key words: implantation, decidualization, fertility, angiogenesis, mouse model, pregnancy, uterus.

Introduction

Infertility is a common reproductive health disorder in humans and affects about 10%–15% of reproductive aged couples worldwide [1]. Only 50%–60% of all conceptions advance beyond 20 weeks of gestation and implantation failure is the major cause of early pregnancy loss, reaching about 75% [2]. Assisted reproductive technologies (ART) have helped millions with fertility issues [3]. Despite the significant improvements in culture medium and embryo quality, the success rate of ART remains low mainly due to implantation failure [4]. Therefore, it is imperative to gain a comprehensive understanding of the mechanism underlying implantation to address this global clinical issue. Many studies have identified molecules and proteins that are critical during embryo implantation, but the mechanisms regulating implantation are not still fully understood [5–7].

Embryo implantation is the process whereby the mature blastocyst attaches and then penetrates into the maternal endometrium to begin forming the placenta [8]. It is a mandatory step for reproduction in mammals and requires synchronized development of the embryo and the uterus, as well as highly organized communication between the two [9]. The luminal epithelium is the first maternal cell layer that an embryo attaches to, and is a key gateway for embryo implantation and subsequent embryo development [6]. After attachment, the embryo must penetrate through the luminal epithelium and the basement membrane. The luminal epithelial cells at the implantation site undergo specific changes such as controlled disassembly of adhesive complexes and apoptosis to assist the invasion of the embryo [10]. The embryo then needs to break through the basement membrane, which is a specialized extracellular scaffold composed of type IV collagen, laminin, perlecan, peroxidasin, and nidogen [11–13]. It is a contiguous layer prior to implantation and becomes disrupted at the site of implantation. Once the removal of the luminal epithelium and the basement membrane have occurred, the trophoblast and stromal cells come into close contact and further development of the pregnancy continues.

After implantation, the stromal cells surrounding the embryo undergo a proliferation and differentiation process known as decidualization [5]. Decidualization is a prerequisite for successful pregnancy because it provides the implanted embryo with growth factors and cytokines, controls the implantation window and selection of embryos, establishes the local immune microenvironment at the fetal-maternal interface, maintains tissue homeostasis during trophoblast invasion, protects the embryo from inflammation and reactive oxygen species, and supports the angiogenesis processes to nourish the growing embryo as well as promotes formation of the placenta [1, 14–17]. This critical morphological and functional transformation is dependent upon the action of the steroid hormone progesterone, epithelial cell secreted factors, cell cycle regulators, transcription factors, and immune cells [14, 18–20]. Many genes and signaling pathways have been identified to play a role in decidualization. For example, progesterone promotes Bone morphogenetic protein 2 (*Bmp2*), which stimulates its downstream target Wingless-related integration site 4 (*Wnt4*) to promote decidualization. Loss of either *Bmp2* or *Wnt4* leads to failure of decidualization and infertility [21, 22]. In addition, BMP2 also regulates the cell cycle transcription factor CCAAT enhancer-binding protein beta (CEBPB), which acts via the Signal transducer and activator of transcription 3 (STAT3) pathway to modulate decidualization. Mice with conditional deletion of CEBPB and STAT3 in the uterus also show decidualization defects [23, 24]. Development of genetically engineered mouse models has provided a wealth of information about the signaling pathways in implantation and decidualization.

Basigin (BSG) is a transmembrane glycoprotein that belongs to the immunoglobulin superfamily [25]. It is expressed in many cell and tissue types and is involved in different physiological functions [26]. BSG is also expressed in the reproductive organs of humans and mice and is essential for successful fertility in both males and females [27–29]. In female mice, BSG is expressed in the embryo, ovary, and the uterus. On Day 1 of pregnancy, BSG is expressed in the luminal and glandular epithelium, and by Day 4 of pregnancy, it is expressed in the stromal cells. Following implantation, BSG is expressed in the secondary decidual zone and eventually in the undifferentiated stromal cells [28, 30]. Limited global knockout studies

have shown that female mice lacking BSG are profoundly infertile [31, 32]. However, global knockout of *Bsg* is highly embryonic lethal, making it difficult to study the role of BSG in reproduction. Among the few mice that survive to adulthood, they are also more susceptible to develop pneumonia and neurological disorders [33–35]. However, the role of *Bsg* in implantation and decidualization remains unclear. To bypass the embryonic lethality caused by global deletion of *Bsg*, we generated a tissue specific *Bsg* knockout mouse model using the progesterone receptor (PR)-Cre and loxP system to study the function of BSG in female reproduction. In this study, we hypothesized that uterine expression of *Bsg* is required for normal fertility and aimed to elucidate the roles of *Bsg* in the uterus during pregnancy. Here we demonstrate that conditional deletion of Bsg in the female reproductive tract results in subfertility due to uterine defects throughout pregnancy. Specifically, we demonstrate that absence of uterine Bsg results in impaired implantation, reduced uterine receptivity and decidualization and reduced angiogenesis in the uterus.

Material and methods

Generation and genotyping of Bsg conditional knockout mice

To generate the *Bsg* cKO mice, we made a *Bsg* floxed C57/BL6 mouse where two loxP sites were inserted into the genome, flanking exon 1 of the *Bsg* gene ($Bsg^{f/f}$) (Supplemental Figure 1). We then crossed this mouse line with a Cre recombinase containing C57/BL6 line described by Soyal et al. [36]. Then $Bsg^{f/f}$ and $PR^{+/+}$ female mice were crossed with $Bsg^{f/f}$ and $PR^{cre/+}$ male mice, to generate $Bsg^{f/f}$ and $PR^{cre/+}$ (conditional *Bsg* knockout, cKO) and $Bsg^{f/f}$ and $PR^{+/+}$ (littermate control) female offspring. Genotypes were determined by PCR and DNA gel electrophoresis. Briefly, DNA from mouse tail tip was extracted with extraction solution (Sigma E7526) at 55°C for 3 min, with addition of neutralization buffer (Sigma N3910). Then 2 µl of DNA solution were added to 10 µl of Red Extract-N-Amp PCR Ready Mix buffer (Sigma R4775) and primer sets for a total volume of 20 µl PCR mix for each sample. The DNA was amplified by PCR using a thermal cycler for 30 cycles. After PCR, DNA was loaded on a 1% agarose gel containing 1 µl of ethidium bromide and run by electrophoresis at 120 V for 60 min. A LSM4000 Image Quant system was used to visualize the DNA and determine the genotypes of the mice. All mice were housed at the University of Illinois at Urbana-Champaign, Institute for Genomic Biology Animal Facility in polysulfone cages. Food (Harlan Teklad 8604) and filtered water were provided for the mice ad libitum. The room was maintained at a temperature of 22 ± 1°C and on a 12-hour light–dark cycle. All experimental procedures including animal care, surgery, euthanasia, and tissue collection were approved by the Institutional Animal Care and Use Committee at the University of Illinois at Urbana–Champaign.

Fertility study

A 6-month fertility study was carried out to determine whether the cKO females experienced subfertility or infertility. Eight female mice at 2-months of age for each genotype were housed individually with one wild type male mouse of proven fertility continuously for 6 months. During this time, mice were checked daily for pregnancy and parturition. Fertility outcomes including the number of litters born per female, the number of pups born per litter, the pup weight and pup sex were recorded and analyzed. These mice were used only for observation of litter size and frequency.

Tissue collection and histological processing

Female mice of each genotype were bred with wild type males at 2 months of age. The day of a vaginal plug was designated as Day 1 of pregnancy. On pregnancy Day 1, 4, 5, 6, 9, 12, and 15, mice were euthanized by CO_2 to collect uterine tissue. One uterine horn was snap frozen in liquid nitrogen and stored at −80°C for RNA extraction. The other uterine horn was fixed in 10 ml of 10% buffered formalin for 24 h, transferred into 70% ethanol and processed for histology as described before [37]. The uterine tissues were processed in a VipTek tissue processor, embedded with paraffin into 5 mm thick blocks and then sectioned into 5 µm thick sections using a microtome. The slides were dried for at least 24 h before being processed for further analysis.

Serum progesterone level analysis

Serum samples were collected for progesterone measurement on Day 4 of pregnancy. Briefly, blood was drawn immediately after euthanasia from the posterior vena cava and cooled on ice for 30 min, then 15 min at room temperature (RT) to clot. The samples were centrifuged at 1000 × g for 10 min to remove the clot, and the supernatant liquid component (serum) was subjected to an enzyme-linked immunosorbent assay (ELISA) using a commercially available progesterone ELISA kit (DRG EIA1561) for quantifying progesterone levels. The kit has a sensitivity of 0.0045 ng/ml and detects progesterone ranges from 0 to 40 ng/ml.

Superovulation

To assess ovarian response to hormonal stimuli and ovulation in the cKO mice, a superovulation experiment was performed. Nine mice of each genotype were injected *ip* with 6 IU of pregnant mare serum gonadotropin (PMSG, Prospec HOR-272) at 3 p.m. on Day 1. The mice were rested for 2 days before receiving 6 IU of human chorionic gonadotropin (HCG, Millipore #230734) 46 h later at 1 p.m. on Day 3. After superovulation, the mice were euthanized the next day (Day 4) at 10 a.m. to collect the oviducts. Oviducts were transferred to the lab, and were gently pierced at the ampulla region to release a cloud of oocytes in a complex with cumulus cells. The oocytes were first incubated in 500 µl of PBS with 20 µl of hyaluronidase (Sigma H4272) for 20 min to remove the excess cumulus cells. The oocytes were then transferred to a new petri dish with a drop of PBS and then imaged by a light microscope to count the number harvested from each mouse.

Embryo flushing

The number of embryos reaching the uterine horn at the time of implantation was determined by flushing embryos from the uteri on Day 4 of pregnancy from both cKO and control mice. Seven female mice of each genotype were individually housed with one wild type male of known fertility. On Day 4 of pregnancy, mice were euthanized, and the uterine horns were collected. A 1 ml syringe with 30-gauge needle was used to flush the embryos by injecting 1 ml of PBS into each uterine horn. The flushing was repeated three times to ensure flushing of all embryos. The number of embryos was determined using a light microscope and photographic images were taken to evaluate the development stages of the embryos.

RNA isolation and quantitative reverse transcription-PCR

Total RNA was extracted from uterine tissues from mice on Day 4 and Day 5 of pregnancy or from artificial decidualization response (ADR) deciduoma using the Qiagen RNeasy Mini kit (Qiagen #74104) according to the manufacturer's instructions. The concentration of mRNA was determined by a nanodrop and the quality of the mRNA was assessed using the Bioanalyzer at the Functional Genomics Center at the University of Illinois, Urbana-Champaign (https://biotech.illinois.edu/functionalgenomics). One microgram of total RNA was reverse transcribed using the First Strand cDNA Synthesis Kit from Roche (#4379012001) following the manufacturer's instructions. After cDNA was synthesized, quantitative reverse transcription-PCR (qRT-PCR) was performed to assess the mRNA levels of decidualization and other gene markers in the uteri and decidua of the mice using Power Sybr Green Master Mix (Life Tech A25742). Briefly, 5 µl of a 1:7 diluted cDNA sample were mixed with 10 µl of master mix (7.5 µl of Sybr Green Mix, 0.6 µl primer sets, and 1.9 µl of water) for a total volume of 15 µl per well in a MicroAmp optical 384-well reaction plate. Three technical replicates were performed for each sample. qRT-PCR amplification and quantitation were performed using a Quant Studio (Applied Biosytem) from the Functional Genomics Center. The reaction was run for 40 cycles (95°C for 15 s, 60°C for 1 min). The comparative CT method (ΔΔCT) was used for quantification of gene expression. Relative fold changes in gene expression for all tested genes were normalized to Peptidylprolyl isomerase A(*Ppia)* and Ribosomal protein, large, P0 (*Rplp0)* endogenous housekeeping genes. Genes analyzed include *Bsg*, *Cebpb*, *Bmp2*, *Wnt4*, heart and neural crest derivatives-expressed protein 2 (*Hand2*), Alkaline phosphatase (*Alph*), and Epiregulin encoding gene (*Ereg*). The primer sequences of these genes are listed in Supplemental Table 1.

Immunohistochemical and immunofluorescence staining

Immunohistochemistry (IHC) was performed for BSG on samples collected on Day 1, 4, and 6 of pregnancy as previous described [38]. Briefly, slides of uterine horns were deparaffinized using three xylenes and rehydrated though a series of decreasing concentrations of ethanol, then subjected to heat-induced antigen retrieval with DAKO Target Retrieval Solution at 1:10 dilution (10× pH 9) (Dako Denmark A/S, Denmark, Part Number: S236784-2, Code: S2367) at 100°C for 30 min and allowed to cool to RT. This was followed by inactivation of endogenous peroxidase activity with 0.3% H_2O_2/methanol for 15 min in the dark. The samples were then rinsed with phosphate buffered saline with Tween-20 (PBST) and incubated in blocking solution consisting of 5% horse serum (Vectastain ABC kit, Vector Laboratories, Inc. Burlingame, CA, USA) diluted in 1%BSA/PBST at RT for 60 min. The tissue sections were incubated with primary antibodies overnight at 4°C. The primary antibodies used were: BSG (1:200; R&D system AF772), LIF (1:200; Origene, TA321468), PR (1:500; DAKO), CEBPβ (1:100; Santa Cruz sc-150), HAND2 (1:200; Abcam ab200040), and KI67 (1:200; Abcam ab833). The negative control sections were incubated in a nonspecific IgG of the same species as the primary antibodies to confirm specificity of the primary antibodies. Next day, slides were rinsed with PBST prior to incubation with antigoat biotinylated secondary antibody (Vectastain ABC kit, Vector Laboratories, Inc. Burlingame, CA, USA) at 1:200 dilution in PBST for 60 min at RT. Slides were then rinsed and incubated in ABC solution (PBS: A: B = 50:1:1) (Vectastain ABC kit, Vector Laboratories, Inc. Burlingame, CA, USA) for 30 min at RT. For visualization of the immunoreactivity, all slides were subjected to chromogen 3′3-diaminobenzidine (DAB) (Vector Laboratories, Inc. Burlingame, CA, USA) for 30 s. Slides were rinsed in tap water for 10 min to stop the DAB reaction. Thereafter, the slides were counterstained with hematoxylin for 1 min followed by dehydration and cover-slipping. After drying for 24 h, the slides were cleaned and loaded into a Hamamatsu Nanozoomer 2.0 HT for scanning.

For immunofluorescence (IF) staining, uterine slides were deparaffinized and underwent antigen retrieval using the same methods as for IHC. Slides were then incubated in blocking solution consisting of 5% horse serum (Vectastain ABC kit, Vector Laboratories, Inc. Burlingame, CA, USA) diluted in 1%BSA/PBST at RT for 60 min. The tissue sections were incubated with a primary antibody in blocking solution at specific concentrations overnight at 4°C. The primary antibodies used were: BSG (1:200; R&D system AF772), monocarboxylate transporter 1 (MCT1) (1:100; LSBio c335287), E-cadherin (1:100; R&D system af748), pan cytokeratin (1:200; Sigma c2562), and CD31 (1:50; Abcam, ab28364). The negative control sections were incubated with the same concentration of a nonspecific IgG of the same species as the primary antibodies to confirm specificity of the primary antibodies. On the following day, slides were rinsed with PBST prior to incubation with either an antigoat Alexa488 conjugated secondary antibody (Jackson Immuno Research # 805-545-180), an antirabbit Cy3 conjugated secondary antibody (Jackson Immuno Research # 711-165-152) or an antimouse Cy5 conjugated secondary antibody (Jackson Immuno Research # 715175151) in PBST at 1:200 dilution for 1 h at RT. After incubation, slides were rinsed with PBS and covered with a DAPI containing mounting medium (Vector Laboratories, H-1200). To detect the immunoreactivity, all slides were imaged using a Zeiss LSM 710 confocal microscope at the Institute for Genomic Biology at the University of Illinois, Urbana-Champaign.

Jones' silver stain

Jones' silver stain was performed to assess the integrity of the uterine basement membrane. Briefly, slides of uterine horns on Day 5 were deparaffinized using three xylenes and rehydrated through a series of decreasing concentrations of ethanol, and then oxidized in 0.5% periodic acid solution for 11 min. After rinsing thoroughly in distilled, deionized water, slides were placed in freshly made methenamine silver solution (3% methenamine and 5% silver nitrate) at 70°C for 60 min. The slides were checked every 20 min for precipitate formation. Once a medium brown color stain appeared, slides were rinsed in distilled deionized water at 70°C. The slides were then placed in 0.2% gold chloride solution for 1 min, rinsed in distilled water and treated with sodium thiosulfate for 1 min. The slides were then rinsed in running tap water for 10 min before counterstaining. Fast green (Fisher) was used for 1 min as a counterstain. The slides were then dehydrated and covered. After drying for 24 h, the slides were cleaned and loaded into a Hamamatsu Nanozoomer 2.0 HT for scanning.

Artificial decidualization response

The deciduoma forms in response to an artificial deciduogenic stimulus and serves as a well-controlled model of decidualization. To evaluate the decidualization response of the cKO females, an ADR experiment was conducted as previously described [39]. Ten female

mice of each genotype were ovariectomized and rested for 2 weeks to eliminate innate circulating steroid hormones. To precisely control the level of hormones in the animals, 100 ng of estradiol was injected for 3 days, then the mice were rested for 2 days before daily injection of 10 ng estradiol and 1 mg progesterone were administered for another 3 days. On the third day of estradiol and progesterone injection, 15 µl of corn oil (Sigma C8267) were injected into the right uterine horn from the basal part to serve as the deciduogenic stimulus. The other uterine horn was not injected as an internal control. The mice were injected with 1 mg progesterone every day for another 3 days before tissue collection. The uterine horns were weighed separately and photographed at collection. The injected uterine horn (deciduoma) was cut in half. One half was snap frozen in liquid nitrogen for further RNA isolation and qRT-PCR analysis. The other half was fixed in 10% buffered formalin for 24 h, then transferred to 70% ethanol and processed for histological analysis. To measure the size of the cross section of the decidua tissue, H&E stained slides were loaded into a Hamamatsu Nanozoomer 2.0 HT for scanning. The area, perimeter and diameter of the deciduoma cross sections were measured and recorded for each animal.

Statistical analysis

All data were analyzed utilizing GraphPad Prism software 8 (GraphPad Prism, San Diego, CA, USA). Data are presented as means ± standard error of the means. For normally distributed data, unpaired *t* tests were used to compare the control group and the experimental group. For non-normally distributed data, Mann–Whitney tests were used. A statistical significance was assigned at $P \leq 0.05$.

Results

Confirmation of loss of Bsg expression in the uterus of cKO mice

To generate female mice lacking expression of Bsg in uterine cells, we made a $Bsg^{f/f}$ and *PRcre*/+ mouse line in which *Bsg* genomic loci was selectively ablated in PR positive cells (Supplemental Figure 1). Ablation of *Bsg* was confirmed by qPCR and immunohistochemical staining on tissues from mice of both genotypes (Figure 1). Quantitative PCR revealed a 75% reduction in mRNA level of Bsg in whole uteri collected in the cKO mice on Day 4 of pregnancy compared to controls ($n = 4$ each, Student *t*-test, $P < 0.001$) (Figure 1A). Next, we examined the cell type-specific expression of BSG in the uteri on pregnancy Day 1, 4, and 8 as well as in the oviduct (Figure 1B). On Day 1 of pregnancy, BSG was expressed mainly in the luminal epithelial cells and glandular epithelial cells in the control uterus. In the cKO, BSG expression disappeared in the luminal and glandular epithelial cells. On Day 4 of pregnancy, BSG was expressed abundantly in the stromal cells in the control uterus. In the cKO, BSG expression was only detected in endothelial cells and scattered immune cells. On Day 6 of pregnancy, BSG was heavily expressed in the embryo and the secondary decidual zone and undifferentiated stromal cells in the control uterus. In the cKO, BSG expression level was much reduced, occurring mainly in endothelial cells and immune cells in the stroma. The kidney is known to express high levels of BSG and served as a positive control. We observed that the kidneys of cKO females showed extensive BSG expression, confirming that the targeted knockout in PR positive cells was specific.

Deletion of BSG in the uterine cells reduced fertility of female mice

A six-month fertility study was carried out to determine the fertility outcomes of the cKO female mice, and the results are summarized in Table 1. During the 6-month period, the eight cKO females produced 123 pups total, which was 4.56 per litter, and this was significantly smaller than the 309 total pups and 7.73 pups per litter produced by the controls (Figure 2A). The controls produced 40 litters total, which was five litters per female on average. On the other hand, the eight cKO females produced 27 litters total, which was an average of 3.38 litters per female. The litter frequency of the cKO females was significantly smaller than the controls (Figure 2B). Although the cKO mice had fewer pups, the number of dead pups at parturition was much higher than the controls at a 27:7 ratio. Two of the cKO females died due to dystocia and had to be replaced. In addition to the smaller litter frequency and litter size, the fertility decreased much more severely over time in the cKO females compared to the controls (Figure 2C). The controls still produced six pups per litter at their fifth parity, whereas the cKO females produced almost no pups at the fifth parity. This suggests that BSG may play a role in reproductive aging. There was no difference in the pups' weight at birth or sex ratio of the pups between the cKO females and the control females (Supplemental Figure 2).

Uteri from animals with both genotypes were collected on different days of pregnancy. Examples of uteri on Days 6, 9, 12, and 15 of gestation for both cKOs and controls are shown in Figure 2D. For each time point checked, the cKO females had some uteri with implantation failure. In cKO mice with implantation, some had fewer implantation sites, abnormal spacing, or crowded implantation sites. On Days 12 and 15, there were signs of embryo resorption and growth restriction in the cKO females. There were also signs of hemorrhage at implantation sites in the cKO mice. This indicates that pregnancy complications occurred at multiple time points throughout the gestational period and led to a subfertility phenotype in the cKO females.

After carefully checking the pregnancy status of mice at every time point of pregnancy, mice were divided into three groups based on observation of the uteri: 1. No implantation; 2. Abnormal pregnancy, and 3. Normal pregnancy. Only 15.4% of the controls had no implantation and 7.7% had abnormal pregnancies, while the majority of controls had normal pregnancies (76.9%). On the other hand, 25% of the cKO females had no implantation, and 39.3% had abnormal pregnancies. Only 35.7% of the cKO females had normal pregnancies, which was much lower than the controls (Figure 3E).

Ovarian function was normal in Bsg cKO mice

Ovaries are the sources of oocytes and the sites of steroid hormone production, which are critical for reproduction [40]. Ovaries on Day 4 of pregnancy were collected and stained by hematoxylin and eosin to assess morphological differences between the cKO females and the controls (Figure 3A). The ovarian morphology appeared similar between the two genotypes. The cKO ovary had similar number of follicles at different developmental stages as the controls.

To test ovarian function, including ovulation and response to hormones, a superovulation experiment was performed. After stimulating with PMSG and HCG, the cKO females ovulated 16.44 oocytes, which was comparable to the 20.44 oocytes produced by the controls (Figure 3B). The superovulated oocytes were collected and imaged under a light microscope. The morphology and size of the oocytes were similar between the cKOs and the controls (Supplemental Figure 3A).

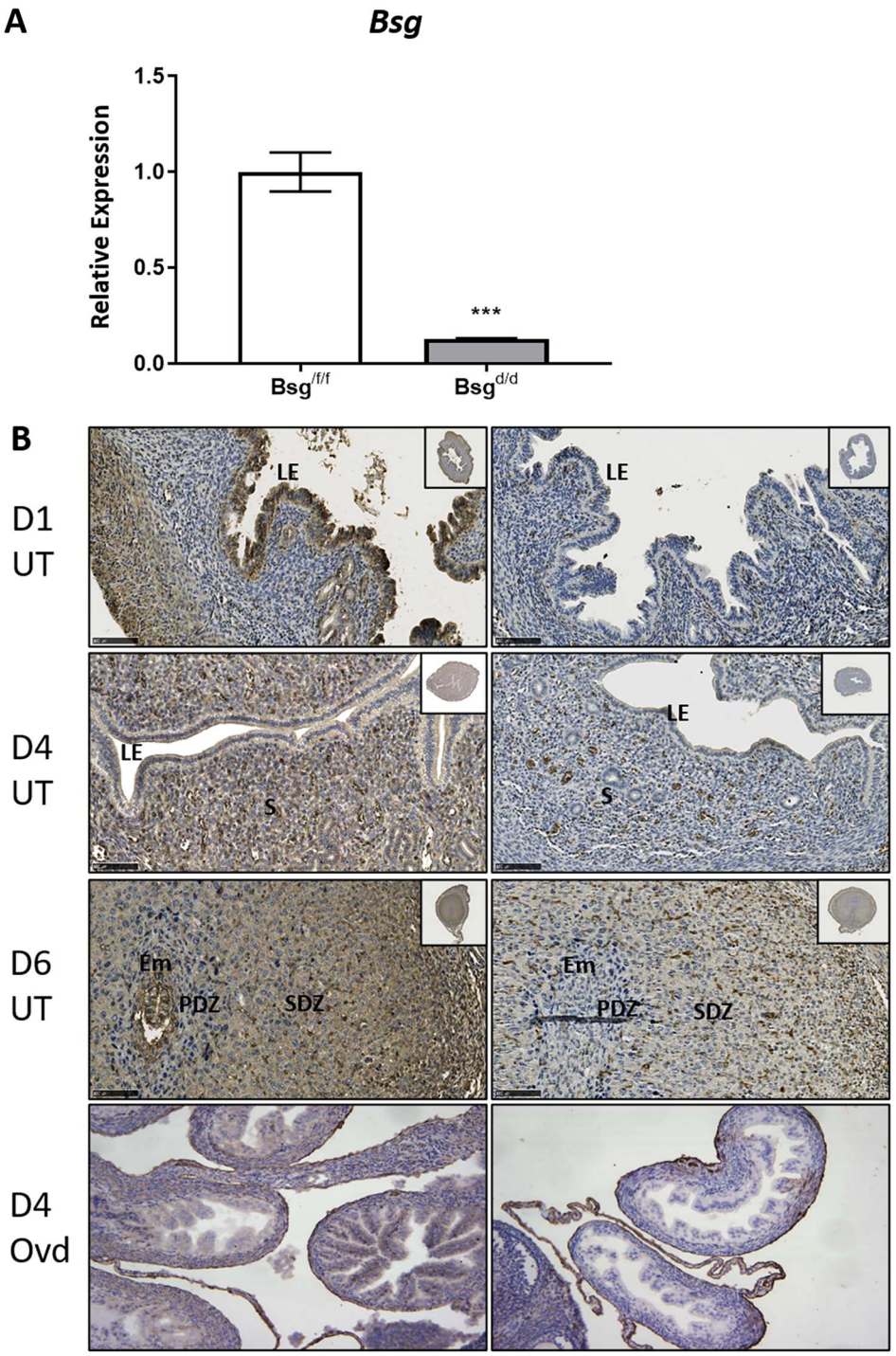

Figure 1. Deletion of *Bsg* in the reproductive tract in female mice. (*A*) Quantitative PCR showed that uteri from cKO mice showed significantly decreased expression of *Bsg* compared with control mice on D4 of pregnancy. $N = 4$ each. $P \leq 0.001$. (*B*) Comparison of immunohistochemical staining for BSG in the uteri on D1 (top panel), D4 (second panel), D6 (third panel) and in the oviduct (bottom panel) in control (left) and cKO (right) mice. LE: luminal epithelium; S: stroma; Em: embryo; PDZ: primary decidual zone; SDZ: secondary decidual zone; UT: uteri; Ovd: oviduct.

Uteri of both genotypes were harvested on the morning of gestational Day 4 and the embryos were flushed and collected. We retrieved an average of 6.29 embryos per mouse from the seven cKO females, which was similar to the 7.86 embryos retrieved from the seven control mice (Figure 3C). After collection, embryos were imaged under a light microscope to evaluate developmental stages. Most of the embryos were at the mature blastocyst stage, or morula stage, regardless of the genotypes of the mother (Supplemental Figure 3B). The cKO females had an average of 0.71 unfertilized or degenerative eggs, which was similar to the 0.43

Table 1. Fertility study results

Genotype	*No. of animals*	*No. of Litters born*	*No. litters per animal*	*No. of pups born*	*No. of pups per litter*	*No. of dead pups*	*Pup weight*
$Bsg^{f/f}$	8	40	*5.0 ± 0.38*	309	*7.73 ± 0.35*	7	1.41 ± 0.01
$Bsg^{d/d}$	8	27	*3.38 ± 0.46**	123	*4.56 ± 0.52**	27	1.38 ± 0.02

Asterisk (*) indicates $P < 0.05$.

unfertilized or degenerative eggs observed in the controls. There were also corpora lutea present in the ovaries of the cKO mice.

Progesterone is a key for maintenance of all events of normal pregnancy [41]. Circulating progesterone levels were measured in serum collected on Day 4 of pregnancy and subjected to progesterone ELISA. The cKO females had 19.12 ng/ml progesterone, which was not different from the 19.35 ng/ml levels measured in the controls (Figure 3D). These data suggest that ovulation, progesterone production, fertilization, and early embryo development were not altered in the cKO mice. Thus, the subfertility of the cKO females was due to uterine defects.

Embryos of Bsg cKO mice failed to penetrate the luminal epithelium and break down the basement membrane

To determine if implantation was impaired in the cKO mice, uterine samples of females of both genotypes were collected on Day 5 of pregnancy. The uterine tissue sections were stained with a pan-cytokeratin antibody (Figure 4A) and the results showed the embryos were marked with green for BSG as they express BSG, whereas the epithelium was marked with red for cytokeratin. In the controls, at the site far away from the embryo, there was continuous expression of cytokeratin, highlighting the luminal epithelium, but at the site of implantation, the expression of cytokeratin was disrupted. However, in the cKO, a significant proportion of the embryos were clearly restrained in the pocket of the epithelial layer.

IF staining of E-cadherin was performed to evaluate the integrity of the luminal epithelium at the implantation site on the evening of Day 5 of pregnancy (Figure 4B). There was no E-cadherin expression in the luminal epithelium at the site of implantation in the control mice, indicating a complete breakdown and apoptosis of the luminal epithelial cells. This suggests the embryos were able to penetrate the luminal epithelial barrier and successfully invade into the stromal layer. However, in a significant proportion (6/9) of the implantation sites of the cKOs examined, the embryos were still surrounded by an intact layer of epithelium with intense E-cadherin expression. The integrity of the epithelium was preserved, indicating failed luminal epithelial breakdown and embryo invasion in the cKO mice. This was assessed on the evening of Day 5, when the embryo should have completed attachment and invasion as the control mice showed [6]. Thus, it suggests that the embryo surrounded by the intact luminal epithelium in cKOs was not due to delayed implantation, but due to incomplete implantation.

The penetration and breakdown of the uterine luminal epithelial basement membrane is required for successful implantation [11]. To assess the status of the basement membrane in the cKO females, Jones' silver stain was performed (Figure 4C) on implantation sites collected on Day 5 evening of pregnancy. In the controls, the black stain lining the luminal epithelium was found away from the embryo, but there was no positive stain at the site of embryo attachment, suggesting a breakdown of the basement membrane. In the cKOs, the black color positive stain was still present at the basal side of the luminal epithelium around the embryo, suggesting an unaltered basement membrane.

Uterine receptivity was impaired in Bsg cKO mice

Successful implantation requires a receptive uterus for the mature blastocyst. The window of receptivity refers to the restricted time that the uterus is capable of accepting the embryo, and it usually lasts around 24 h in mice and 2-3 days in human [42]. To investigate whether uterine receptivity was altered in the cKO, uterine cross sections were stained for PR and LIF at the time of implantation. Our results showed that in the control mouse, PR was expressed exclusively in the stromal cells; however, 3/6 cKO mice had prolonged PR expression in the LE (Figure 5A.) We also observed that in these cKO mice, LIF was expressed in a few stromal cells, but not in the GE cells. On the other hand, LIF was expressed only in the GE cells in the controls (Figure 5B).

We also evaluated the proliferating status of the uterus at the time of implantation. Our results in Supplemental Figure 4 showed that there was no difference in the expression of KI67 in the cKO or control mice on either Day 4 evening or Day 5 morning. KI67 was expressed heavily and exclusively in the stromal cells, indicating proliferation was not altered in the cKO mice.

Decidualization response was impaired in Bsg cKO mice

Proper decidualization is critical for normal pregnancy [1]. An ADR experiment was carried out in both genotypes as described previously. Uteri were photographed at collection and example images are shown in Figure 6A. The results revealed that in the controls, most of the animals displayed a robust response to the stimuli whereas in the cKO mice, there was a very modest response or no response at all in most of the animals. To quantify the size of the decidua, cross sections of the deciduoma were measured (Figure 6B). The area of the controls was 7.2 mm^2, which was significantly higher than the area of the cKOs at 3.86 mm^2. Each uterine horn was weighed and the ratio of injected horn to uninjected horn weight was calculated (Figure 6C). In the controls, on average, the injected uterine horn had a 9.13-fold increase in weight in response to the stimuli. However, in the cKO mice, there was only a modest 2.2-fold increase in the weight of the injected uterine horn, indicating an impaired decidual response. The body weight of each mouse was also measured (Figure 6D). The cKOs weighed 22.73 g on average, which was not different compared to the controls at 23.67 g. This indicates that the differences in the uterine weights between the genotypes of mice were due to different responses to the experimental stimuli, rather than body weight differences.

The expression levels of several decidualization marker genes were evaluated by qRT-PCR in the artificial decidualization model (Figure 6E). The results showed that *Bsg* gene expression levels in the cKO were downregulated by 86% compared to the levels in the

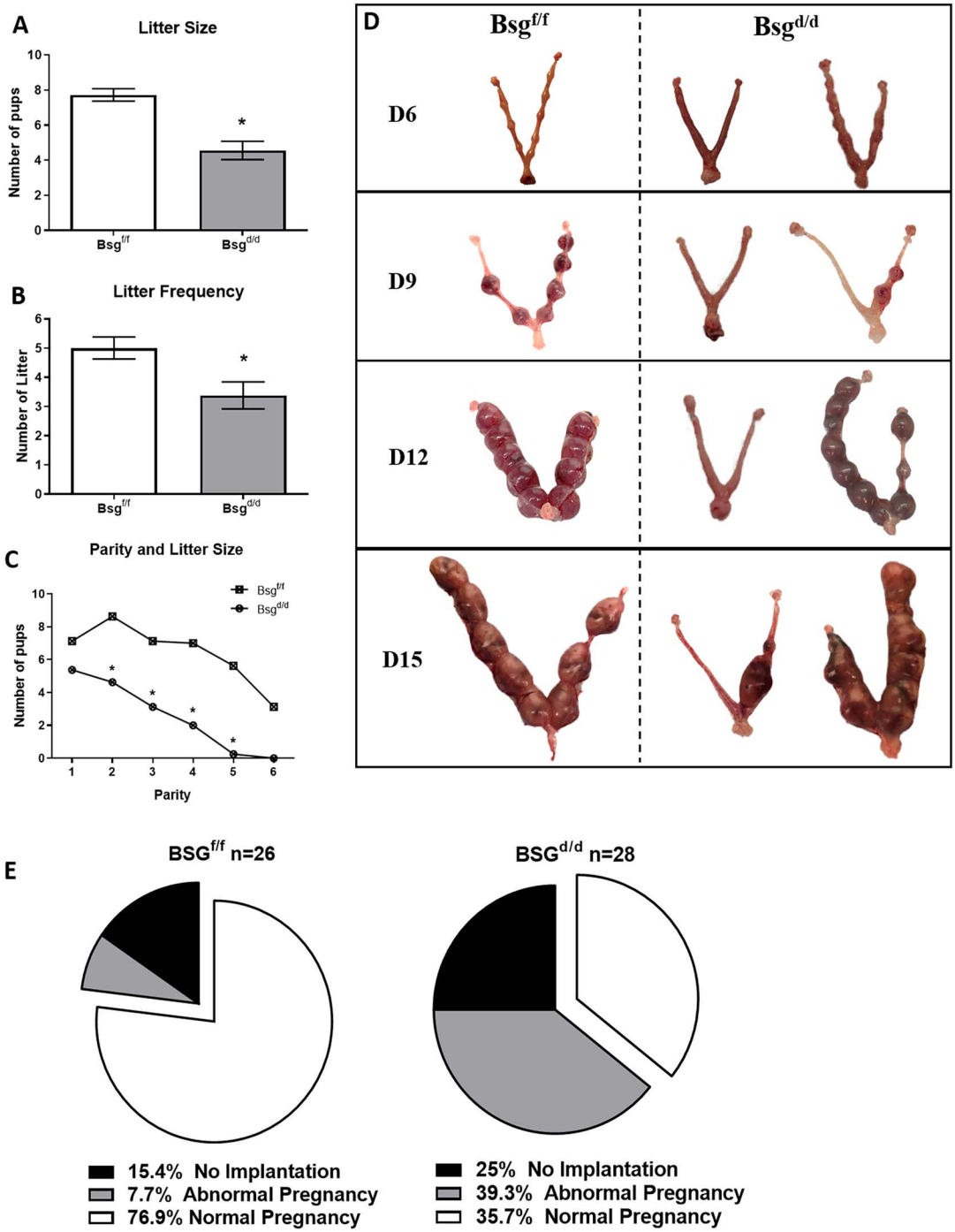

Figure 2. *Bsg* cKO mice exhibited various pregnancy abnormalities and subfertility. *Bsg* cKO mice showed smaller litter size (*A*), litter frequency (*B*), and more severe reduction in fertility in different parities over time (*C*) compared to controls. *Bsg* cKO mice (right) showed implantation failure, embryo resorption and hemorrhage on different gestational days compared to controls (*D*). Evaluation of pregnancy status showed that most cKO mice had either no implantation or abnormal pregnancy (right) compared to controls (left) (*E*).

controls as expected. *Cebpb* expression in the cKOs was significantly downregulated by 75% compared to the levels in the controls and *Bmp2* expression in the cKOs was also significantly downregulated by 88%. These results confirm that specific decidualization marker genes were downregulated in the cKOs, leading to an incomplete decidualization response.

To determine whether the protein expression level was consistent with gene expression level for some of the decidualization genes, CEBPB and HAND2 abundancies were analyzed by IHC. Our results confirmed there was abundant CEBPB protein expression in the deciduoma in the control mice, but little CEBPB expression was evident in the cKO mice (Figure 6F). This confirmed that the

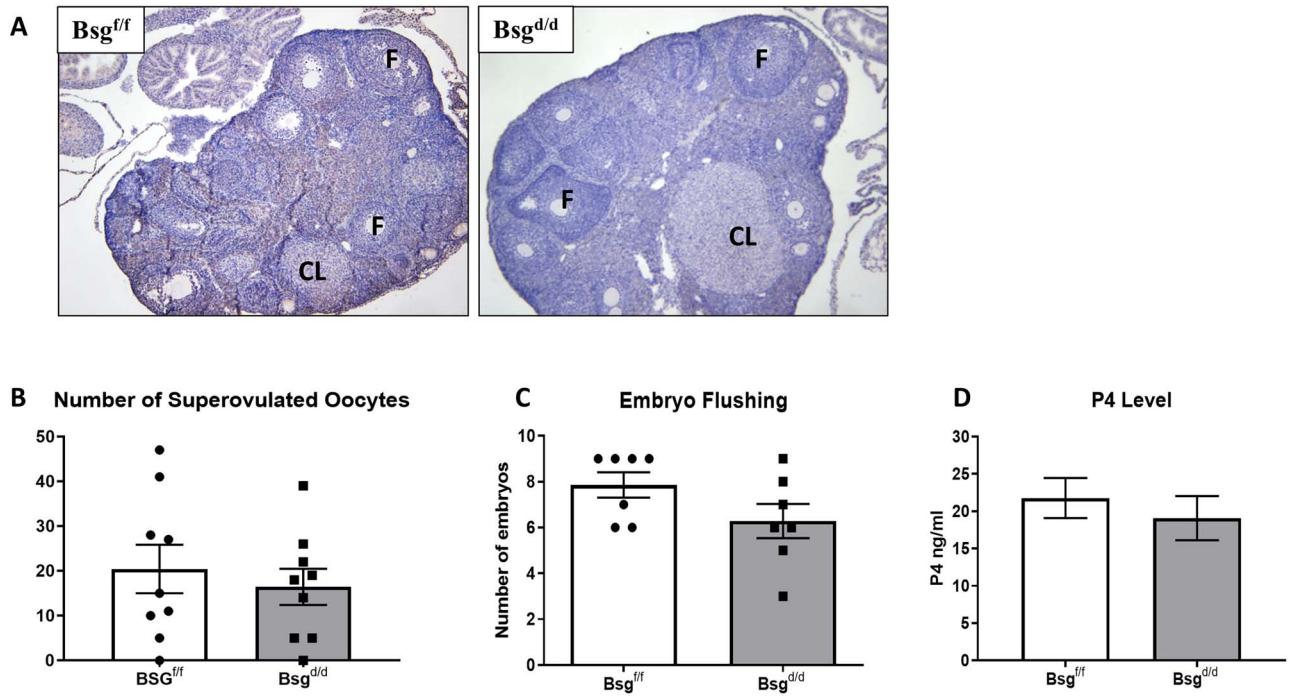

Figure 3. Ovarian function in *Bsg* cKO mice appeared to be normal compared to controls. An ovary of the cKO (right) and control (left) mouse on D4 of pregnancy (*A*). Number of superovulated oocytes (*B*), number of embryos flushed on D4 (*C*) and level of circulating progesterone (*D*) are similar in the control (left) and cKO (right) mice. F: follicle; CL: corpus luteum.

CEBPB protein level was much reduced in the cKOs compared to the controls. Figure 6G shows that in the deciduoma of the controls, HAND2 was abundant in the stromal cells over a wide area. However, in the cKO mice, HAND2 was greatly reduced compared to the controls. Similar results were observed in uteri of Day 5 pregnant mice stained for CEBPB and HAND2. Our results showed that the controls lost E-cadherin expression at the implantation site but had a broad region of stromal cells expressing CEBPB. However, in the cKOs, the expression of CEBPB was limited to a smaller region of stromal cells close to the embryo (Supplemental Figure 5A). HAND2 protein was found in the subepithelial stromal cells surrounding the embryo in the controls. In the cKOs there was some HAND2 in the subepithelial stromal cells, but the area of HAND2 positive cells was much smaller compared to the controls (Supplemental Figure 5B).

MCT1 localization was altered in Bsg cKO mice

MCTs are important for lactate transport and metabolic homeostasis, and MCT1 and MCT4 are shuttled to the membrane by their chaperone protein BSG [43–45]. Uterine sections on Day 6 of pregnancy were stained to assess the abundance and localization of MCT1 in the cKO females. Our results showed that in the controls, BSG was abundant in the deep undifferentiated stromal cells and MCT1 was localized in the same region (B and C). In contrast, BSG was found only in some immune cells and endothelial cells in a scattered pattern within the stroma of the cKO females on Day 6 of pregnancy. MCT1 was very weak at a low magnification, and there was no colocalization of the two proteins (Figure 7A). At a higher magnification focused at the deep stromal layer (Figure 7B), BSG was abundant in the cell membrane in the uteri of the controls. MCT1 was also found in the cell membrane and these two colocalized in the merged image. However, in the cKO females, such colocalization of BSG and MCT1 within the same area was absent. These results confirm that the localization and abundance of MCT1 were altered in the uteri of the cKO females.

Angiogenesis was reduced in Bsg cKO mice

Angiogenesis at the implantation sites was also evaluated in the cKO mice. Uterine sections from Day 6 of pregnancy were stained for the angiogenic marker CD31. Our results showed that, CD31 was abundant in the embryo and in the endothelial cells among deep stromal cells in the controls but was much lower in the cKO mice (Figure 8A). A higher magnification of the deep stromal layer showed clearly that abundance of CD31 was much higher in the controls compared to the cKO females (Figure 8B). To quantify the expression of CD31, images of five fields were randomly selected and quantified for their signal intensity. The results showed that the signal intensity in sections from the controls was 34.92, which was significantly higher than the value of 20.3 in the cKO females (Figure 8C). These results revealed a markedly decreased abundance of CD31 in the uteri of the cKO mice, suggesting reduced angiogenesis at the implantation sites in these animals.

Discussion

BSG is a transmembrane glycoprotein expressed in many tissue and cell types, including the reproductive organs in both humans and mice [28, 46]. In this study, we demonstrated that conditional deletion of *Bsg* in uterine cells resulted in subfertility of the mice, due to the defects we observed at the time of implantation and during decidualization. Work from our group and others has shown that BSG is expressed in the uterus during the estrous cycle and early pregnancy in mice [30, 47]. It is also present in human endometrium and its expression is menstrual cycle-dependent [48, 49]. BSG is expressed in the preimplantation embryos as early as the 2-cell stage

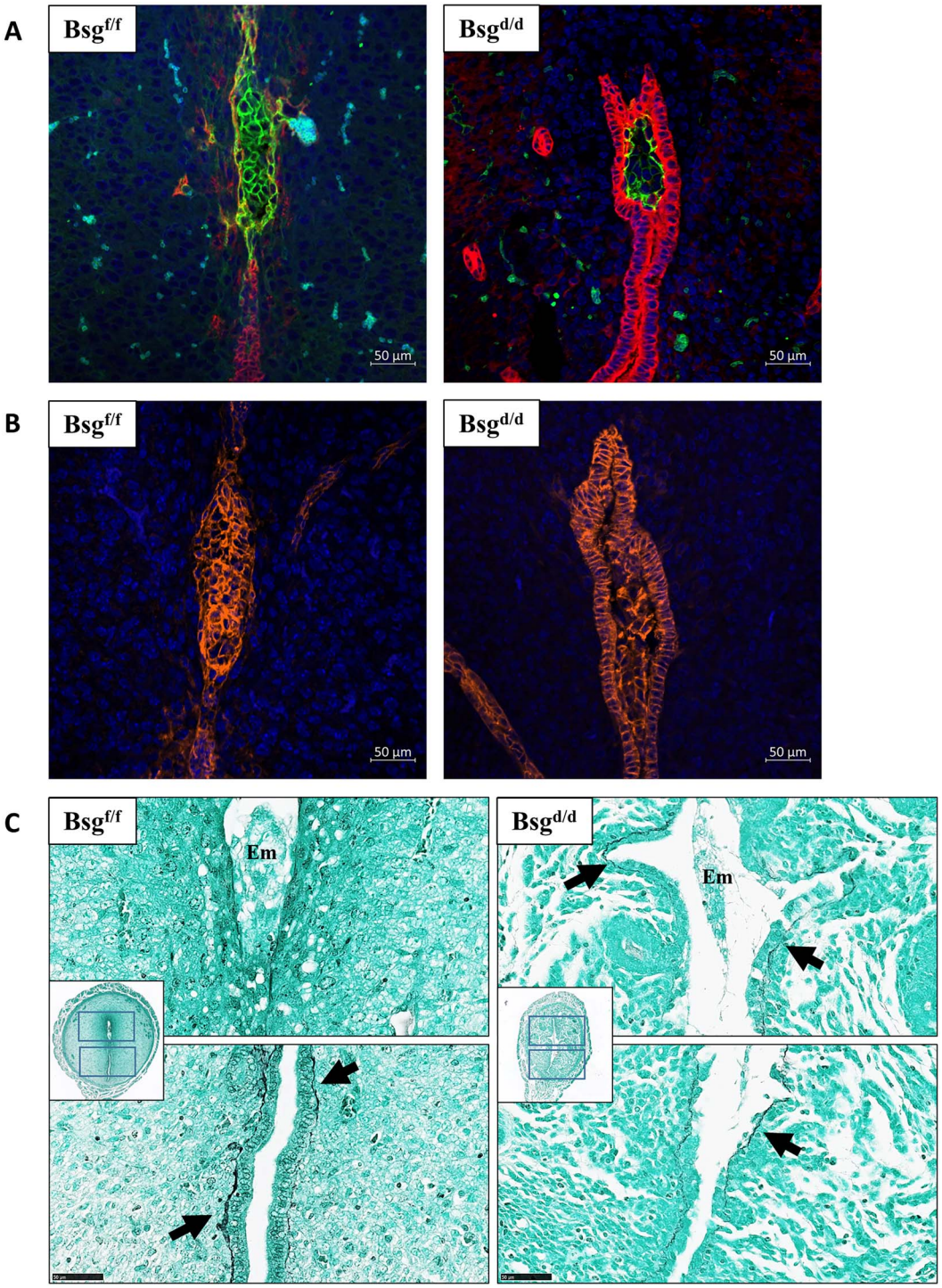

Figure 4. Implantation failed in the Bsg cKO mice. An implantation site of the control (left) and cKO (right) mouse on the evening of D5 (*A* and *B*). Green: BSG; Red: Cytokeratin; Orange: E-cadherin; blue: DAPI. Jones' silver stain on an implantation site of the control (left) and cKO (right) mouse on D5 showing basement membrane (*C*). Arrows indicate positive stain of the basement membrane. Em: embryo.

and is expressed in both the inner cell mass and trophectoderm of mouse blastocysts [28, 31, 50, 51]. Researchers reported that the expression of BSG mRNA is highest in the oocyte, morula, and blastocyst stages [50]. In humans, preimplantation embryos secrete BSG and embryos that developed into blastocysts secreted more BSG than arrested embryos [52]. Bsg is present in the placental trophoblast cells in the first trimester and term placenta in humans [53–55]. It is also expressed in placental trophoblast and endothelial cells throughout gestation in the mouse and rat [56, 57]. Taken together, these data support an important role for Bsg in normal pregnancy.

The results of our 6-month fertility study showed that the cKO females produced markedly smaller litter numbers and litter size compared to the controls, indicating a subfertility phenotype in

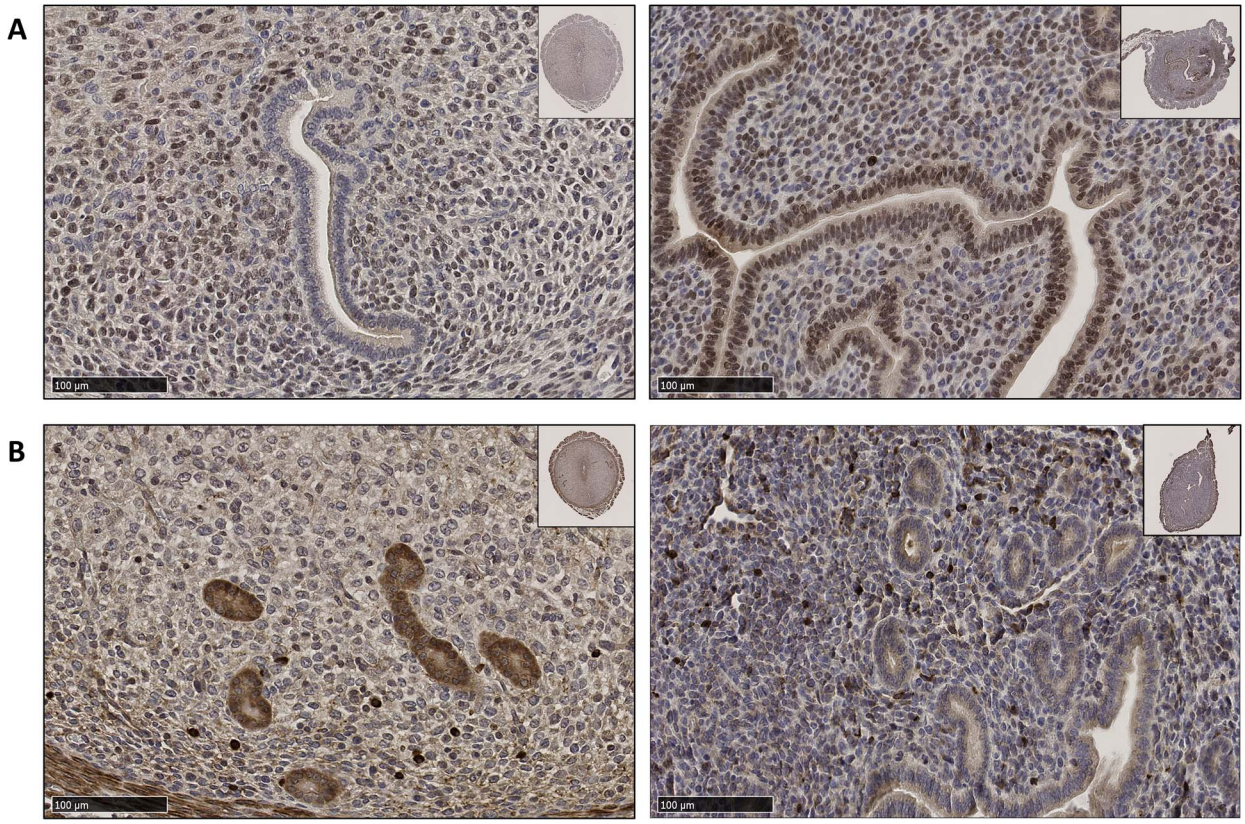

Figure 5. Impaired PR and LIF staining in the Bsg cKO mice. (*A*) An implantation site of the control (left) and cKO (right) mouse stained against PR on D5 morning of pregnancy. PR was still expressed in the LE in the cKO. (*B*) An implantation site of the control (left) and cKO (right) mouse stained against LIF on D5 morning of pregnancy. LIF was expressed in the GE of the control mouse, but not expressed in the GE of the cKO mouse.

cKO mice. Interestingly, we observed that as parity increased, the fertility of the cKOs decreased more severely compared to the controls. Normally, the fertility of animals gradually decreases as they age, however, the age-associated fertility decrease in the cKO mice was accelerated compared to the controls, suggesting a possible role of BSG in reproductive aging. Our results showed no differences in ovarian morphology, number of superovulated oocytes or progesterone levels on Day 4 between the two groups, indicating normal ovarian functions in the cKO mice. This suggested that the reduced fertility in the cKO mice was likely not due to defects in the hypothalamus-pituitary-ovary axis. Indeed, we found uterine defects throughout gestation after assessing pregnancy status at different gestation timepoints. Our results showed that only 15.4% and 7.7% of the controls had no implantation or abnormal pregnancy, respectively, whereas 76.9% had normal pregnancies. However, in the cKO mice, only 35.7% had normal pregnancies. A quarter of the cKO mice had implantation failure and 39.3% had problematic pregnancies. These findings suggest that over the course of pregnancy, BSG may be involved in regulating multiple processes including implantation, decidualization, and placentation. In addition, parturition could likely be affected by the loss of BSG because two cKO mice died due to dystocia and there was a much higher incidence of neonatal death for the cKO mice in the fertility study.

Implantation is a dynamic event that involves a series of physical and physiological interactions between the implanting blastocyst and the receptive uterus [58]. At the time of implantation, the luminal epithelial cells at the implantation site undergo apoptosis and the basement membrane is breached for further invasion of the embryo [59]. During the peri-implantation period, cytokeratin is downregulated in the uterine epithelium of mice, rabbits, and cows [60–62]. Our results showed that the luminal epithelial cells at the site of implantation still expressed cytokeratin in a large proportion of cKO mice on the evening of Day 5 pregnancy. E-cadherin, a $Ca2^{+}$-dependent transmembrane protein that forms adhesion junctions, is also expressed in the luminal epithelium [63]. During implantation, expression of E-cadherin is downregulated due to cell remodeling to assist blastocyst attachment and invasion in mice, rats, and rabbits [60, 64, 65]. Paria et al. reported that E-cadherin is expressed in the luminal epithelium prior to implantation, but that expression is lost during implantation and transiently appears in the stromal cells in mice [64]. Nallasamy et al. showed that persistent expression of E-cadherin results in implantation failure [66]. Our results showed that in a substantial number of the cKO uteri, E-cadherin was expressed throughout the uterine luminal epithelium at the time of implantation. Similarly, activin-like kinase (ALK)-3 cKO mice also expressed E-Cadherin in the luminal epithelium at this time and also experience implantation failure and infertility [67].

A specifically timed window of implantation is required for proper implantation and is regulated by progesterone signaling [42]. Studies have suggested that loss of PR expression in the LE in mice during the preimplantation period is a marker for uterine receptivity, and subsequently this downregulation of PR leads to upregulation of LIF in the GE cells [14, 68]. In our study, the control mice had normal

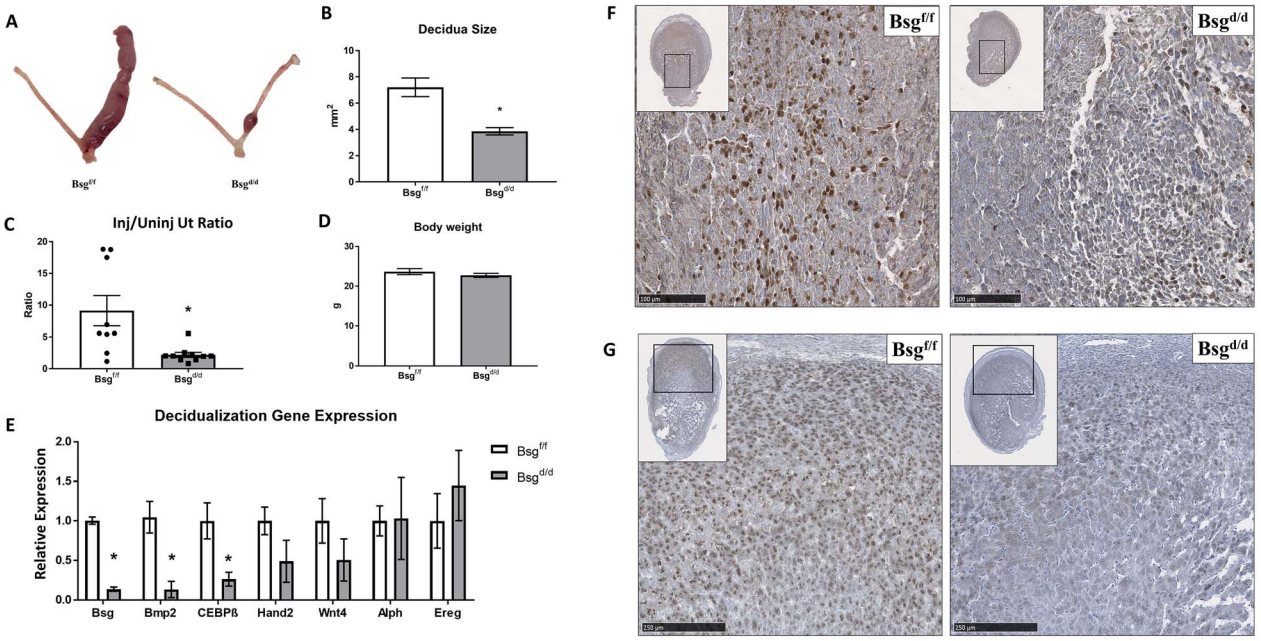

Figure 6. Bsg cKO mice exhibited a compromised decidual response to artificial stimuli. Uterine horns of the cKO mice showed modest decidual response compared to the robust response by the control mice (*A*). The size of uterine cross sections was much smaller in the cKO compared to the control mice (*B*). The stimulated to unstimulated uterine horn weight ratio in the cKO mice was significantly lower than the controls (*C*). The body weight was similar between the cKO and the controls (*D*). Decidualization gene expression levels in the cKO and the control deciduoma (*E*). Immunohistochemical staining showed lower expression of CEBPB (*F*) and HAND2 (*G*) in the cKO compared to the control deciduoma.

stromal expression of PR and glandular epithelial expression of LIF. However, in the cKO mice, 3/6 evaluated implantation sites showed prolonged expression of PR in the LE cells and absence of LIF in the GE cells. This indicates that the receptivity window was altered in some of the cKO mice.

During early pregnancy in rodents and humans, the endometrial stromal cells respond to the invasion of the embryo by undergoing proliferation followed by differentiation; this morphological and functional transformation is known as decidualization. [69]. It is widely accepted that proper decidualization is a prerequisite for successful implantation, and abnormal decidualization can result in implantation failure, miscarriages, preeclampsia, and intrauterine growth restriction [1, 17, 70]. Our results indicated that there was no difference in the proliferation of the uterine stromal cells between the two genotypes. However, in the ADR experiment, we observed that most of the cKO females either did not undergo a decidual response or had only a modest decidual response, whereas the control females had a robust response to the deciduogenic stimulus. The qRT-PCR results showed that *Bmp2* and *Cebpβ* expression in the deciduoma of the cKOs were have been significantly downregulated compared to the controls.

BMP ligands and receptors are expressed in the uterus of pregnant mice, and play key roles in regulating implantation [71]. BMP2 is the most studied and loss of BMP2 in the uterus caused infertility in mice due to failures of embryo attachment and decidualization [67]. BMP2 acts through its receptor ALK2 to regulate decidualization; Alk2 null mice also failed to undergo uterine decidualization [67, 71]. Microarray analysis revealed that CEBPB is downstream of ALK2 and CEBPB expression is suppressed in ALK2 cKO mice. CEBPB is a transcription factor involved in the cell cycle under regulation by steroid hormones, and is expressed in the endometrial stromal cells in mice, baboons, and humans [16, 71–73]. In mice, its expression is rapidly induced at the time of blastocyst attachment, and further increased during decidualization in the proliferating and decidualized stromal cells surrounding the blastocyst. Studies have shown that CEBPB is a key regulator of decidualization as uteri lacking CEBPB failed to undergo decidualization and showed no response to artificial decidualization stimulation similar to our results [74, 75]. CEBPB acts through its direct downstream target STAT3 to regulate the decidual response in human and mice [23, 24]. Interestingly, BSG is reported to promote STAT3 activity in cancer cells [76]. Together with the downregulation of *Bmp2*, this suggests that loss of BSG in the uterus leads to defective decidualization, likely through the BMP-ALK2-CEBPB-STAT3 pathway. Further studies on the expression levels of *Alk2* and *Stat3* should be evaluated to confirm involvement of Bsg in this pathway to regulate decidualization.

HAND2 is a transcription factor that is expressed in uterine stromal cells in mice [77]. Studies have shown that *Hand2* mRNA and protein levels increase in mouse uterine stromal cells during decidualization and this upregulation is embryo independent [78]. Reduction of *Hand2* expression in these cells using RNA knock down leads to reduced decidualization in both mouse and human stromal cells in vitro [78]. The results of our studies showed that both mRNA and protein abundance of HAND2 were downregulated in the deciduoma from the ADR experiment and in the uteri on Day 5 of pregnancy in the cKO mice compared to the controls. Our findings indicate that loss of BSG in the mouse uterus leads to compromised decidualization through downregulation of *Hand2* expression.

Angiogenesis during implantation is crucial for pregnancy establishment and maintenance [4]. The differentiating stromal cells form an avascular primary decidual zone on Day 5 surrounding the

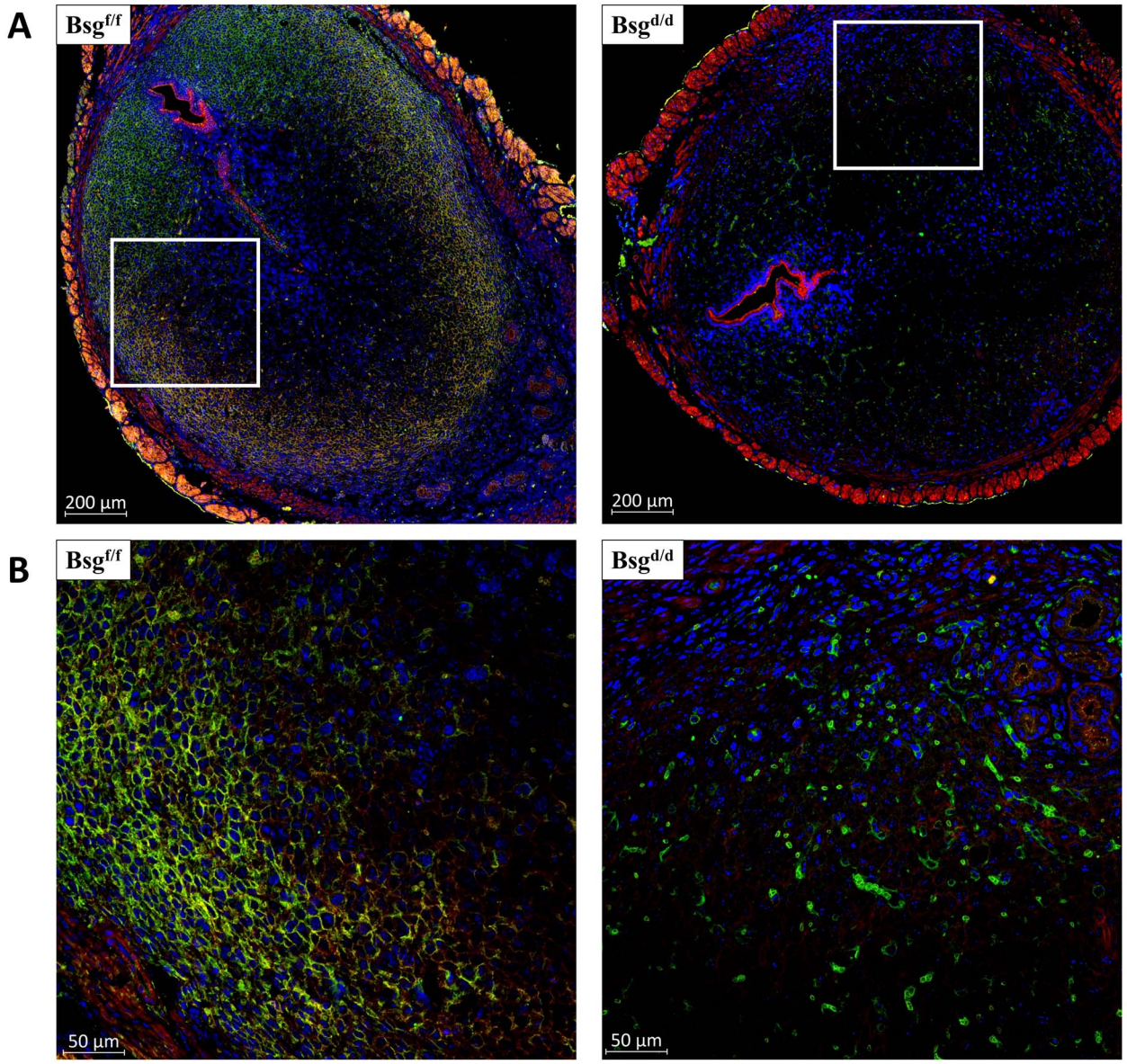

Figure 7. Bsg cKO mice showed altered MCT1 expression on D6 of pregnancy. A uterine cross section of a control (left) and cKO (right) mouse stained for BSG and MCT1 (*A*: low magnification; *B*: high magnification). Green: BSG; red: MCT1; blue: DAPI.

embryos, and then form a well vascularized secondary decidual zone by Day 8 [79]. BSG is important in promoting angiogenesis as studies have shown that BSG overexpression promotes tumor angiogenesis and growth by inducing vascular endothelial growth factors (VEGFs) and matrix metalloproteinases (MMPs) expression in both human and mouse [80]. We observed a significant reduction in the presence of the angiogenic marker CD31 in the uteri of cKO mice on Day 6 of pregnancy. This observation is very similar to a study examining the role of gap junction protein connexin 43 (Cx43) in female reproduction, where the Cx43 cKO mice were subfertile due to failed decidualization [81]. Loss of Cx43 also caused a striking impairment in angiogenesis with a reduction in the expression of CD31 and VEGF [81]. Our findings indicate that loss of *Bsg* leads to reduced angiogenesis in the cKO females. Future studies investigating the effects of loss of *Bsg* on the expression of connexins and VEGFs in the cKO mice are warranted.

In this study, six out of nine cKO mice examined on Day 5 evening of pregnancy had implantation failure and 70% of the cKO mice had no decidual response or only a modest response to the artificial decidualization stimuli. Thus, not all the cKO mice were negatively affected by deleting *Bsg* in uterine cells during pregnancy. There are potentially several explanations for the range in severity of the subfertility phenotype in the cKO mice. First, PR is not expressed in all uterine compartment and cell types. Studies have shown that PR is expressed in the luminal and glandular epithelial cells, stromal cells, and myometrium of cycling mice, with only PRB in the luminal epithelium, and both PRA and PRB in the stroma and myometrium [82, 83]. It is worth noting that not all stromal cells express PR. Soyal et al. reported that some stromal cells did not possess Cre activity when characterizing the PR-Cre and Lox mouse model [36, 84]. The second possibility is that the PR negative cells in the uterus still express BSG and this is enough BSG to maintain some level of fertility

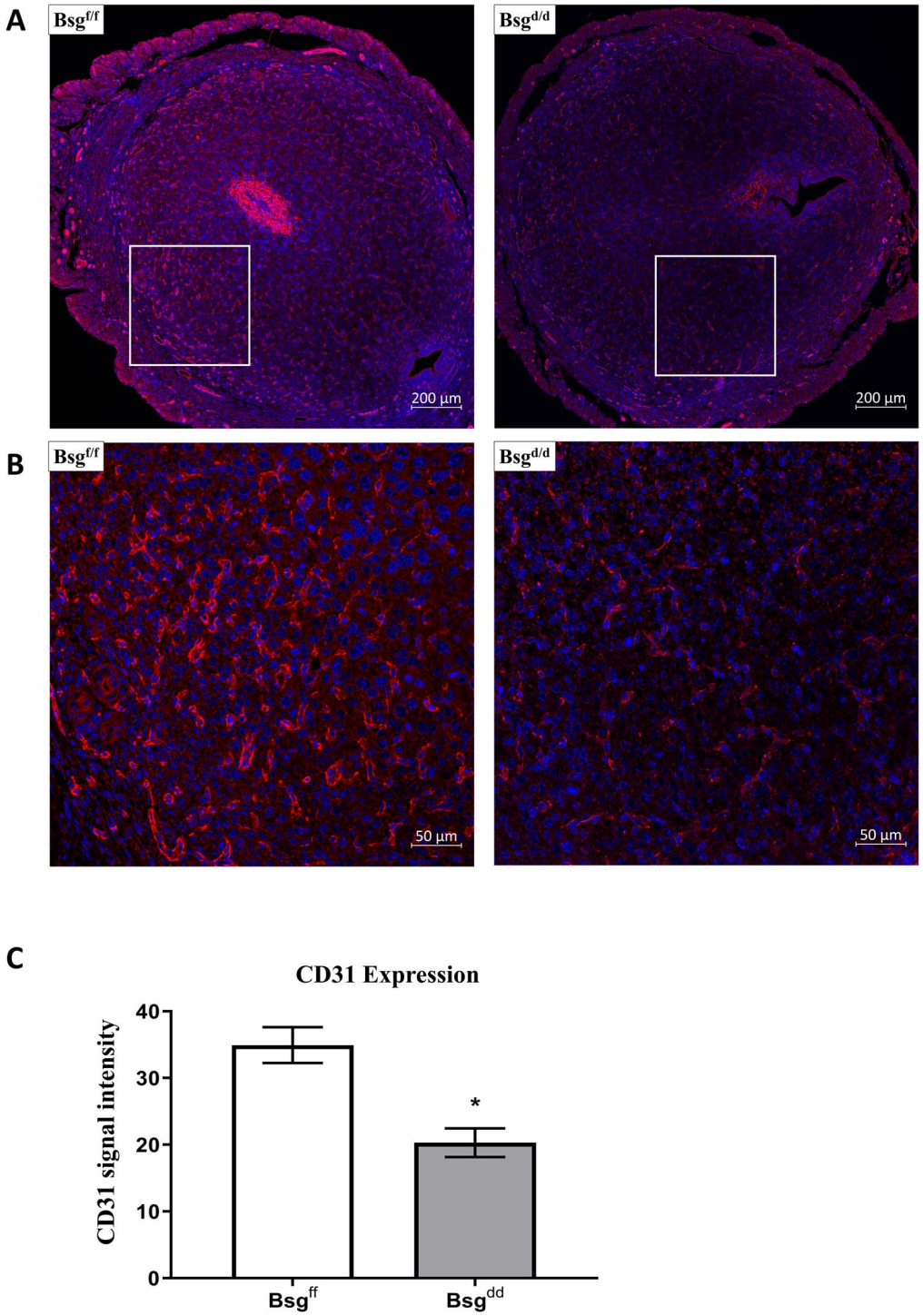

Figure 8. Bsg cKO mice showed reduced angiogenesis in the stroma on D6 of pregnancy. A uterine cross section of a control (left) and cKO (right) mouse stained for CD31 (*A*: low magnification; *B*: high magnification). Red: CD31; blue: DAPI. CD31 intensity was significantly lower in the cKO uteri compared to the controls (*C*).

in the cKO animals. Endothelial cells and certain immune cells such as macrophages express BSG, but are PR negative [25, 84, 85]. These cells could provide BSG function through paracrine activity. In addition, studies have shown that BSG is present in microvesicles and can be released through microvesicle shedding [85–88]. Thus, it is important to investigate whether microvesicles shed by the embryo, endothelial or immune cells in the cKO mice contain BSG. A third possible explanation is a compensatory mechanism of BSG related molecules. Embigin, the founding member of the Ig superfamily, is expressed in the uterus and acts as an ancillary protein when BSG is absent [89]. For example, MCT1 and MCT4 have highest affinity for binding BSG, but when BSG is absent, they can also bind

to embigin. Thus, the effectiveness of the PR knockout, paracrine activity or microvesicle shedding by BSG producing cells, as well as compensatory effects by embigin could potentially explain the range of subfertility caused by loss of uterine BSG using this PR-Cre mouse model.

MCTs are short-chain fatty acids transporters for lactate, pyruvate, and ketone bodies and play an important role in metabolic homeostasis in many tissue types including the uterus [43]. BSG is a chaperone protein for MCT1 and MCT4 and is responsible for shuttling these MCTs to the plasma membrane [44, 45, 90]. MCT1 and BSG colocalize and form a heterodimer through its transmembrane domain that is critical for cells with a high glycolytic rate under hypoxic conditions. The increase in glycolytic flux is also seen in physiological processes with rapidly proliferating cells such as in embryo implantation [30, 91]. Our IF results showed that MCT1 expression and localization were altered in the cKO mice compared to the controls. Silencing of *Bsg* in human malignant melanoma cells or in lung fibroblast cells abrogated the expression of MCT1 and downregulated glycolysis [92, 93]. Therefore, lactate transport in the stromal cells of cKO mice needs to be investigated.

In conclusion, we have shown that deletion of *Bsg* in the female reproductive tract leads to subfertility in mice. Mice lacking *Bsg* exhibit impaired implantation, compromised decidualization, reduced uterine angiogenesis, hemorrhage, and embryo growth restriction. Future studies will focus on in vitro studies to investigate decidualization, MMP secretion, and lactate production under hypoxic conditions.

Data availability statement

The data underlying this article are available in the article and in its online supplementary material.

Supplementary material

Supplementary material is available at *BIOLRE* online.

Authors' contributions

KL and RAN designed the study. KL and SB performed experiments. KL and RAN analyzed the data and wrote the paper. QL and BMB contributed expertise. All authors edited and reviewed the manuscript.

Acknowledgments

We would like to thank the Institute for Genomic Biology core facility for providing equipment and expertise for imaging. We thank Dr CheMyong Jay Ko for providing aliquots of PR antibody that has now been discontinued by Dako. We also thank Karen Doty for her assistance in histology analysis.

Conflict of interest: The authors have no conflict of interest.

References

1. Ramathal C, Bagchi I, Taylor R, Bagchi M. Endometrial decidualization: Of mice and men. *Semin Reprod Med* 2010; **28**:17–26.
2. Norwitz E, Schust D, Fisher S. Implantation and the survival of early pregnancy. *N Engl J Med* 2001; **345**:1400–1408.
3. Sharkey AM, Smith SK. The endometrium as a cause of implantation failure. *Best Pract Res Clin Obstet Gynaecol* 2003; **17**:289–307.
4. Zhang S, Lin H, Kong S, Wang S, Wang H, Wang H, Armant DR. Physiological and molecular determinants of embryo implantation. *Mol Aspects Med* 2013; **34**:939–980.
5. Cha J, Dey SK, Lim H. *Embryo Implantation, Physiology of Reproduction: Two-Volume Set*, vol. **2**, 4th ed. Elsevier Inc.; 2014.
6. Ye X. Uterine luminal epithelium as the transient gateway for embryo implantation. *Trends Endocrinol Metab* 2020; **31**:165–180.
7. Aplin JD, Ruane PT. Embryo-epithelium interactions during implantation at a glance. *J Cell Sci* 2017; **130**:15–22.
8. Aplin JD, Kimber SJ. Trophoblast-uterine interactions at implantation. *Reprod Biol Endocrinol* 2004; **2**:48.
9. J. Cha, X. Sun, and S. K. Dey, "Mechanisms of implantation: Strategies for successful pregnancy," *Nat Med*, vol. **18**, Nature Publishing Group, pp. 1754–1767, 2012.
10. Parr EL, Tung HN, Parr MB. Apoptosis as the mode of uterine epithelial cell death during embryo implantation in mice and Rats1. *Biol Reprod* 1987; **36**:211–225.
11. Blankenship TN, Given RL. Loss of laminin and type IV collagen in uterine luminal epithelial basement membranes during blastocyst lmplantation in the mouse. *Anat Rec* 1995; **243**:27–36.
12. Fisher SJ, Leitch MS, Kantor MS, Basbaum CB, Kramer RH. Degradation of extracellular matrix by the trophoblastic cells of first-trimester human placentas. *J Cell Biochem* 1985; **27**:31–41.
13. Jones-Paris CR, Paria S, Berg T, Saus J, Bhave G, Paria BC, Hudson BG. Embryo implantation triggers dynamic spatiotemporal expression of the basement membrane toolkit during uterine reprogramming. *Matrix Biol* 2017; **57–58**:347–365.
14. Wetendorf M, DeMayo FJ. The progesterone receptor regulates implantation, decidualization, and glandular development via a complex paracrine signaling network. *Mol Cell Endocrinol* 2012; **357**:108–118.
15. Monsivais D, Clementi C, Peng J, Fullerton PT Jr, Prunskaite-Hyyryläinen R, Vainio SJ, Matzuk MM. BMP7 induces uterine receptivity and blastocyst attachment. *Endocrinology* 2017; **158**:979–992.
16. Bhurke AS, Bagchi IC, Bagchi MK. Progesterone-regulated endometrial factors controlling implantation. *Am J Reprod Immunol* 2016; **75**:237–245.
17. Singh M, Chaudhry P, Asselin E. Bridging endometrial receptivity and implantation: Network of hormones, cytokines, and growth factors. *J Endocrinol* 2011; **210**:5–14.
18. Conneely OM, Mulac-Jericevic B, Lydon JP. Progesterone-dependent regulation of female reproductive activity by two distinct progesterone receptor isoforms. *Steroids* 2003; **68**:771–778.
19. Das SK. Cell cycle regulatory control for uterine stromal cell decidualization in implantation. *Reproduction* 2009; **137**:889–899.
20. Croy BA, Chen Z, Hofmann AP, Lord EM, Sedlacek AL, Gerber SA. Imaging of vascular development in early mouse decidua and its association with leukocytes and Trophoblasts1. *Biol Reprod* 2012; **87**:1–11.
21. Lee KY, Jeong JW, Wang J, Ma L, Martin JF, Tsai SY, Lydon JP, DeMayo FJ. Bmp2 is critical for the murine uterine decidual response. *Mol Cell Biol* 2007; **27**:5468–5478.
22. Franco HL, Dai D, Lee KY, Rubel CA, Roop D, Boerboom D, Jeong JW, Lydon JP, Bagchi IC, Bagchi MK, DeMayo FJ. WNT4 is a key regulator of normal postnatal uterine development and progesterone signaling during embryo implantation and decidualization in the mouse. *FASEB J* 2011; **25**:1176–11187.
23. Cheng JG, Chen JR, Hernandez L, Alvord WG, Stewart CL. Dual control of LIF expression and LIF receptor function regulate Stat3 activation at the onset of uterine receptivity and embryo implantation. *Proc Natl Acad Sci USA* 2001; **98**:8680–8685.
24. Wang W, Taylor RN, Bagchi IC, Bagchi MK. Regulation of human endometrial stromal proliferation and differentiation by C/EBPβ involves cyclin E-cdk2 and STAT3. *Mol Endocrinol* 2012; **26**:2016–2030.
25. Xin X, Zeng X, Gu H, Li M, Tan H, Jin Z, Hua T, Shi R, Wang H. CD147/EMMPRIN overexpression and prognosis in cancer: A systematic review and meta-analysis. *Sci Rep* 2016; **113**:1–12.
26. Li K, Nowak RA. The role of basigin in reproduction. *Reproduction* 2020; **159**:R97–R109.

27. Braundmeier AG, Dayger CA, Mehrotra P, Belton RJ, Nowak RA. EMMPRIN is secreted by human uterine epithelial cells in microvesicles and stimulates metalloproteinase production by human uterine fibroblast cells. *Reprod Sci* 2012; **19**:1292–1301.
28. Chen L, Nakai M, Belton RJ, Nowak RA. Expression of extracellular matrix metalloproteinase inducer and matrix metalloproteinases during mouse embryonic development. *Reproduction* 2007; **133**:405–414.
29. Bi J, Li Y, Sun F, Saalbach A, Klein C, Miller DJ, Hess R, Nowak RA. Basigin null mutant male mice are sterile and exhibit impaired interactions between germ cells and Sertoli cells. *Dev Biol* 2013; **380**:145–156.
30. Chen L, Belton RJ, Nowak RA. Basigin-mediated gene expression changes in mouse uterine stromal cells during implantation. *Endocrinology* 2009; **150**:966–976.
31. Igakura T, Kadomatsu K, Kaname T, Muramatsu H, Fan QW, Miyauchi T, Toyama Y, Kuno N, Yuasa S, Takahashi M, Senda T, Taguchi O et al. A null mutation in basigin, an immunoglobulin superfamily member, indicates its important roles in peri-implantation development and spermatogenesis. *Dev Biol* 1998; **194**:152–165.
32. Kuno N, Kadomatsu K, Fan QW, Hagihara M, Senda T, Mizutani S, Muramatsu T. Female sterility in mice lacking the basigin gene, which encodes a transmembrane glycoprotein belonging to the immunoglobulin superfamily. *FEBS Lett* 1998; **425**:191–194.
33. Naruhashi K, Kadomatsu K, Igakura T, Fan QW, Kuno N, Muramatsu H, Miyauchi T, Hasegawa T, Itoh A, Muramatsu T, Nabeshima T. Abnormalities of sensory and memory functions in mice lacking Bsg gene. *Biochem Biophys Res Commun* 1997; **236**:733–737.
34. Igakura T, Kadomatsu K, Taguchi O, Muramatsu H, Kaname T, Miyauchi T, Yamamura KI, Arimura K, Muramatsu T. Roles of basigin, a member of the immunoglobulin superfamily, in behavior as to an irritating odor, lymphocyte response, and blood-brain barrier. *Biochem Biophys Res Commun* 1996; **224**:33–36.
35. Muramatsu T, Miyauchi T. Basigin (CD147): A multifunctional transmembrane protien involved in reproduction, neural function, inflammation and tumor invasion. *Histol Histopathol* 2003; **18**:981–987.
36. Soyal SM, Mukherjee A, Lee KYS, Li J, Li H, DeMayo FJ, Lydon JP. Cre-mediated recombination in cell lineages that express the progesterone receptor. *Genesis* 2005; **41**:58–66.
37. Li K, Liszka M, Zhou C, Brehm E, Flaws JA, Nowak RA. Prenatal exposure to a phthalate mixture leads to multigenerational and transgenerational effects on uterine morphology and function in mice. *Reprod Toxicol* 2020; **93**:178–190.
38. Salem W, Li K, Krapp C, Ingles SA, Bartolomei MS, Chung K, Paulson RJ, Nowak RA, McGinnis LK. Imatinib treatments have long-term impact on placentation and embryo survival. *Sci Rep* 2019; **9**:2535.
39. Bany BM, Harvey MB, Schultz GA. Expression of matrix metalloproteinases 2 and 9 in the mouse uterus during implantation and oil-induced decidualization. *J Reprod Fertil* 2000; **120**:125–134.
40. M. Jamnongjit and S. R. Hammes, "Ovarian steroids: The good, the bad, and the signals that raise them," *Cell Cycle*, vol. **5**, Taylor and Francis Inc., pp. 1178–1183, 2006.
41. Terakawa J, Watanabe T, Obara R, Sugiyama M, Inoue N, Ohmori Y, Hosaka YZ, Hondo E. The complete control of murine pregnancy from embryo implantation to parturition. *Reproduction* 2012; **143**:411–415.
42. S. P. Wu, R. Li, and F. J. DeMayo, "Progesterone receptor regulation of uterine adaptation for pregnancy," *Trends Endocrinol Metab*, vol. **29**, Elsevier Inc., pp. 481–491, 2018.
43. Halestrap AP. The monocarboxylate transporter family-structure and functional characterization. *IUBMB Life* 2012; **64**:1–9.
44. Woodhead VE, Stonehouse TJ, Binks MH, Speidel K, Fox DA, Gaya A, Hardie D, Henniker AJ, Horejsi V, Sagawa K, Skubitz KM, Taskov H et al. Novel molecular mechanisms of dendritic cell-induced T cell activation. *Int Immunol* 2000; **12**:1051–1061.
45. Gallagher SM, Castorino JJ, Wang D, Philp NJ. Monocarboxylate transporter 4 regulates maturation and trafficking of CD147 to the plasma membrane in the metastatic breast cancer cell line MDA-MB-231. *Cancer Res* 2007; **67**:4182–4189.
46. Fossum S, Mallett S, Neil Barclay A. The MRC OX-47 antigen is a member of the immunoglobulin superfamily with an unusual transmembrane sequence. *Eur J Immunol* 1991; **21**:671–679.
47. Xiao LJ, Diao HL, Ma XH, Ding NZ, Kadomatsu K, Muramatsu T, Yang ZM. Basigin expression and hormonal regulation in the rat uterus during the peri-implantation period. *Reproduction* 2002; **124**:219–225.
48. Noguchi Y, Sato T, Hirata M, Hara T, Ohama K, Ito A. Identification and characterization of extracellular matrix metalloproteinase inducer in human endometrium during the menstrual cycle in vivo and in vitro. *J Clin Endocrinol Metab* 2003; **88**:6063–6072.
49. Braundmeier AG, Fazleabas AT, Nowak RA. Extracellular matrix metalloproteinase inducer expression in the baboon endometrium: Mestrual cycle and endometriosis. *Reproduction* 2010; **140**:911–920.
50. Ding N-Z, He C-Q, Yang Z-M. Quantification of basigin mRNA in mouse oocytes and preimplantation embryos by competitive RT-PCR. *Zygote* 2002; **10**:239–243.
51. Hérubel F, El Mouatassim, Guérin P, Frydman R, Ménézo Y. Genetic expression of monocarboxylate transporters during human and murine oocyte maturation and early embryonic development. *Zygote* 2002; **10**:175–181.
52. Lindgren KE, Gülen Yaldir F, Hreinsson J, Holte J, Kårehed K, Sundström-Poromaa I, Kaihola H, Åkerud H. Differences in secretome in culture media when comparing blastocysts and arrested embryos using multiplex proximity assay. *Ups J Med Sci* 2018; **123**:143–152.
53. Li W, Alfaidy N, Challis JRG. Expression of extracellular matrix metalloproteinase inducer in human placenta and fetal membranes at term labor. *J Clin Endocrinol Metab* 2004; **89**:2897–2904.
54. Wang Y, Mi S, Li J, Wang Y, Shang T. Differential expression of extracellular matrix metalloproteinase inducer in normal placenta and preeclampsia placenta. *Zhonghua Fu Chan Ke Za Zhi* 2006; **41**:436–439.
55. Lee CL, Lam MPY, Lam KKW, Leung CON, Pang RTK, Chu IK, Wan THL, Chai J, Yeung WSB, Chiu PCN. Identification of CD147 (basigin) as a mediator of trophoblast functions. *Hum Reprod* 2013; **28**:2920–2929.
56. Dang Y, Li W, Tran V, Khalil RA. EMMPRIN-mediated induction of uterine and vascular matrix metalloproteinases during pregnancy and in response to estrogen and progesterone. *Biochem Pharmacol* 2013; **86**:734–747.
57. Nagai A, Takebe K, Nio-Kobayashi J, Takahashi-Iwanaga H, Iwanaga T. Cellular expression of the monocarboxylate transporter (MCT) family in the placenta of mice. *Placenta* 2010; **31**:126–133.
58. Wang H, Dey SK. Roadmap to embryo implantation: Clues from mouse models. *Nat Rev Genet* 2006; **7**:185–199.
59. Pampfer S, Donnay I. Apoptosis at the time of embryo implantation in mouse and rat. *Cell Death Differ* 1999; **6**:533–545.
60. Gou J, Hu T, Li L, Xue L, Zhao X, Yi T, Li Z. Role of epithelial-mesenchymal transition regulated by twist basic helix-loop-helix transcription factor 2 (Twist2) in embryo implantation in mice. *Reprod Fertil Dev* 2019; **31**:932–940.
61. Olson GE, Winfrey VP, Blaeuer GL, Palisano JR, Nagdas SK. Stage-specific expression of the intermediate filament protein cytokeratin 13 in luminal epithelial cells of secretory phase human endometrium and Peri-implantation stage rabbit endometrium 1. *Bio Reprod* 2002; **66**:1006–1015.
62. Haeger JD, Hambruch N, Dantzer V, Hoelker M, Schellander K, Klisch K, Pfarrer C. Changes in endometrial ezrin and cytokeratin 18 expression during bovine implantation and in caruncular endometrial spheroids in vitro. *Placenta* 2015; **36**:821–831.
63. Wesseling J, Van Der Valk, Hilkens J. A mechanism for inhibition of E-cadherin-mediated cell-cell adhesion by the membrane-associated mucin episialin/MUC1. *Mol Biol Cell* 1996; **7**:565–577.
64. Paria BC, Zhao X, Das SK, Dey SK, Yoshinaga K. Zonula occludens-1 and E-cadherin are coordinately expressed in the mouse uterus with the initiation of implantation and decidualization. *Dev Biol* 1999; **208**:488–501.
65. Li Q, Wang J, Armant DR, Bagchi MK, Bagchi IC. Calcitonin down-regulates E-cadherin expression in rodent uterine epithelium during implantation. *J Biol Chem* 2002; **277**:46447–46455.

66. Nallasamy S, Li Q, Bagchi MK, Bagchi IC. Msx homeobox genes critically regulate embryo implantation by controlling paracrine signaling between uterine stroma and epithelium. *PLoS Genet* 2012; **8**:e1002500.
67. Monsivais D, Clementi C, Peng J, Titus MM, Barrish JP, Creighton CJ, Lydon JP, DeMayo FJ, Matzuk MM. Uterine ALK3 is essential during the window of implantation. *Proc Natl Acad Sci* 2016; **113**:E387–E395.
68. Wetendorf M, Wu SP, Wang X, Creighton CJ, Wang T, Lanz RB, Blok L, Tsai SY, Tsai MJ, Lydon JP, DeMayo FJ. Decreased epithelial progesterone receptor A at the window of receptivity is required for preparation of the endometrium for embryo attachment. *Biol Reprod* 2017; **96**:313–326.
69. Peng S, Li J, Miao C, Jia L, Hu Z, Zhao P, Li J, Zhang Y, Chen Q, Duan E. Dickkopf-1 secreted by decidual cells promotes trophoblast cell invasion during murine placentation. *Reproduction* 2008; **135**:367–375.
70. Kong S, Aronow BJ, Handwerger S. Gene expression microarray data analysis of decidual and placental cell differentiation. *Methods Mol Med* 2006; **121**:425–438.
71. Clementi C, Tripurani SK, Large MJ, Edson MA, Creighton CJ. Activin-like kinase 2 functions in Peri-implantation uterine signaling in mice and humans. *PLoS Genet* 2013; **9**:1003863.
72. Wang W, Li Q, Bagchi IC, Bagchi MK. The CCAAT/enhancer binding protein is a critical regulator of steroid-induced mitotic expansion of uterine stromal cells during decidualization. *Endocrinology* 2010; **151**:3929–3940.
73. Kannan A, Fazleabas AT, Bagchi IC, Bagchi MK. The transcription factor C/EBPβ is a marker of uterine receptivity and expressed at the implantation site in the primate. *Reprod Sci* 2010; **17**:434–443.
74. M. K. Bagchi, S. R. Mantena, A. Kannan, and I. C. Bagchi, "Control of uterine cell proliferation and differentiation by C/EBPβ: Functional implications for establishment of early pregnancy," *Cell Cycle*, vol. **5**, Taylor and Francis Inc., pp. 922–925, 2006.
75. Mantena SR, Kannan A, Cheon Y-P, Li Q, Johnson PF, Bagchi IC, Bagchi MK. CEBP is a critical mediator of steroid hormone-regulated cell proliferation and differentiation in the uterine epithelium and stroma. Proc Natl Acad Sci USA 2006; **103**:1870–1875.
76. Li L, Tang W, Wu X, Karnak D, Meng X, Thompson R, Hao X, Li Y, Qiao XT, Lin J, Fuchs J, Simeone DM et al. HAb18G/CD147 promotes pSTAT3-mediated pancreatic cancer development via CD44s. *Clin Cancer Res* 2013; **19**:6703–6715.
77. Li Q, Kannan A, DeMayo FJ, Lydon JP, Cooke PS, Yamagishi H, Srivastava D, Bagchi MK, Bagchi IC. The antiproliferative action of progesterone in uterine epithelium is mediated by hand2. *Science (80-)* 2011; **331**:912–916.
78. Huyen BBDV. Evidence for a conserved function of heart and neural crest derivatives expressed transcript 2 in mouse and human decidualization. *Reproduction* 2011; **142**:353–368.
79. Wang X, Matsumoto H, Zhao X, Das S, Paria B. Embryonic signals direct the formation of tight junctional permeability barrier in the decidualizing stroma during embryo implantation. *J Cell Sci* 2004; **117**:53–62.
80. Tang Yi, Nakada MT, Kesavan P, Mccabe F, Millar H, Rafferty P, Bugelski P, Yan, Li. Extracellular matrix metalloproteinase inducer stimulates tumor angiogenesis by elevating vascular endothelial cell growth factor and matrix metalloproteinases. *Cancer Res* 2005; **65**: 3193–3199.
81. Laws MJ, Taylor RN, Sidell N, DeMayo FJ, Lydon JP, Gutstein DE, Bagchi MK, Bagchi IC. Gap junction communication between uterine stromal cells plays a critical role in pregnancy-associated neovascularization and embryo survival. *Development* 2008; **135**:2659–2668.
82. Binder AK, Winuthayanon W, Hewitt SC, Couse JF, Korach KS. Knobil and Neil's Physiology of Reproduction: Two-Volume Set. *Steroid Receptors in the Uterus and Ovary*, vol. **1**, 4th ed. Elsevier; 2014.
83. Mote PA, Arnett-Mansfield RL, Gava N, deFazio A, Mulac-Jericevic B, Conneely OM, Clarke CL. Overlapping and distinct expression of progesterone receptors A and B in mouse uterus and mammary gland during the estrous cycle. *Endocrinology* 2006; **147**:5503–5512.
84. Ismail PM, Li J, DeMayo FJ, O'Malley BW, Lydon JP. A novel lacZ reporter mouse reveals complex regulation of the progesterone receptor promoter during mammary gland development. *Mol Endocrinol* 2002; **16**:2475–2489.
85. Hahn JN, Kaushik DK, Yong VW. The role of EMMPRIN in T cell biology and immunological diseases. *J Leukoc Biol* 2015; **98**:33–48.
86. Nabeshima K, Iwasaki H, Koga K, Hojo H, Suzumiya J, Kikuchi M. Emmprin (basigin/CD147): Matrix metalloproteinase modulator and multifunctional cell recognition molecule that plays a critical role in cancer progression. *Pathol Int* 2006; **56**:359–367.
87. Sidhu SS, Mengistab AT, Tauscher AN, LaVail J, Basbaum C. The microvesicle as a vehicle for EMMPRIN in tumor–stromal interactions. *Oncogene* 2004; **23**:956–963.
88. Emilova V. *Basigin in Trophoblast Cells Via Microvesicle Shedding Viktoriya thesis*. University of Illinois Urbana Champaign; 2012.
89. Nakai M, Chen L, Nowak RA. Tissue distribution of basigin and monocarboxylate transporter 1 in the adult male mouse: A study using the wild-type and basigin gene knockout mice. *Anat Rec - Part A Discov Mol Cell Evol Biol* 2006; **288**:527–535.
90. Amit-Cohen B-C, Rahat MAMM, Rahat MAMM. Tumor cell-macrophage interactions increase angiogenesis through secretion of EMMPRIN. *Front Physiol* 2013; **4**:178.
91. Bougatef F, Quemener C, Kellouche S, Naïmi B, Podgorniak MP, Millot G, Gabison EE, Calvo F, Dosquet C, Lebbé C, Menashi S, Mourah S. EMMPRIN promotes angiogenesis through hypoxia-inducible factor-2α–mediated regulation of soluble VEGF isoforms and their receptor VEGFR-2. *Blood* 2009; **114**:5547–5556.
92. Su J, Chen X, Kanekura T. A CD147-targeting siRNA inhibits the proliferation, invasiveness, and VEGF production of human malignant melanoma cells by down-regulating glycolysis. *Cancer Lett* 2009; **273**: 140–147.
93. le Floch R, Chiche J, Marchiq I, Naiken T, Ilc K, Murray CM, Critchlow SE, Roux D, Simon MP, Pouyssegur J. CD147 subunit of lactate/H+ symporters MCT1 and hypoxia-inducible MCT4 is critical for energetics and growth of glycolytic tumors. *Proc Natl Acad Sci USA* 2011; **108**:16663–16668.